HHS Public Access

Author manuscript

Mol Cancer Res. Author manuscript; available in PMC 2016 May 01.

Published in final edited form as:

Mol Cancer Res. 2015 May ; 13(5): 828–838. doi:10.1158/1541-7786.MCR-15-0016-T.

The lncRNA *DRAIC/PCAT29* locus constitutes a tumor suppressive nexus

Kouhei Sakurai[1], **Brian J. Reon**[1], **Jordan Anaya**[1], and **Anindya Dutta**[1]

[1]Department of Biochemistry and Molecular Genetics, University of Virginia School of Medicine, Charlottesville, VA, 22908, USA

Abstract

Long non-coding RNAs (lncRNAs) are emerging as major regulators of cellular phenotypes and implicated as oncogenes or tumor suppressors. Here we report a novel tumor suppressive locus on human chromosome 15q23 that contains two multi-exonic lncRNA genes of 100 kb each: *DRAIC* (*LOC145837*) and the recently reported *PCAT29*. The *DRAIC* lncRNA was identified from RNA-seq data and is downregulated as prostate cancer cells progress from an androgen dependent (AD) to castration resistant (CR) state. Prostate cancers persisting in patients after androgen deprivation therapy (ADT) select for decreased *DRAIC* expression, and higher levels of *DRAIC* in prostate cancer is associated with longer disease-free survival (DFS). Androgen induced androgen receptor (AR) binding to the *DRAIC* locus and repressed *DRAIC* expression. In contrast, FOXA1 and NKX3-1 are recruited to the *DRAIC* locus to induce *DRAIC*, and FOXA1 specifically counters the repression of *DRAIC* by AR. The decrease of FOXA1 and NKX3-1, and aberrant activation of AR, thus accounts for the decrease of *DRAIC* during prostate cancer progression to the CR state. Consistent with *DRAIC* being a good prognostic marker, *DRAIC* prevents the transformation of cuboidal epithelial cells to fibroblast-like morphology and prevents cellular migration and invasion. A second tumor suppressive lncRNA *PCAT29*, located 20 kb downstream of *DRAIC*, is regulated identically by AR and FOXA1 and also suppresses cellular migration and metastasis. Finally, based on TCGA analysis, *DRAIC* expression predicts good prognosis in a wide range of malignancies: bladder cancer, low grade gliomas, lung adenocarcinoma, stomach adenocarcinoma, renal clear cell carcinoma, hepatocellular carcinoma, skin melanoma and stomach adenocarcinoma.

Implications—This study reveals a novel tumor suppressive locus encoding two hormone-regulated lncRNAs, *DRAIC* and *PCAT29*, that are prognostic for a wide variety of cancer types.

Keywords

prostate cancer; castration resistance; lncRNA; androgen receptor

Corresponding author: Anindya Dutta, 1340 Jefferson Park Ave, Jordan Hall, Room 1232, Charlottesville, VA, 22908-0733, USA, ad8q@virginia.edu, (434) 924-2466.

Disclosure of Potential Conflicts of Interest: No potential conflicts of interest were disclosed.

Introduction

The growth of prostate cancer cells initially depends on androgen. Therefore, Androgen Deprivation Therapy (ADT) is useful for primary prostate cancer. However, prostate cancer cells progress after ADT to grow in low androgen, a condition called castration resistant (CR) (formerly androgen-independent) state, leading to a tumor recurrence and metastasis (1). Several lines of evidence have shown that the Androgen Receptor (AR) or androgen-responsive pathways are differently activated in the CR cells so that pathways are active in low or absent androgen (1,2) . In addition, alternative pathways such as mTOR and IGF1R signaling are activated to mimic the action of androgens and promote prostate cancer cell growth (3). However, the detailed mechanisms by which androgen dependent (AD) cells become CR remain unclear.

Recent transcriptome analyses have identified a variety of non-coding RNAs as important gene regulators (4–9). Long non-coding RNAs (lncRNAs) are defined as RNAs >200 nt in length with no functional open reading frame (10). Our lab has identified two novel lncRNAs, *APTR* (*Alu*-mediated p21 transcriptional regulator), which recruits PRC2 (Polycomb repressive complex 2) to *p21* promoter region to repress the transcription of *p21* (4) and *MUNC* (MyoD Upstream Non-Coding), which can promote myogenesis (6). Some lncRNAs are known to be aberrantly expressed and act as oncogenes or tumor suppressors in cancers including prostate cancer. Nuclear lncRNAs, *PCGEM1* and *PRNCR1* bind to AR to stimulate AR-mediated gene programs (11). Cytoplasmic lncRNA, *PCAT-1* suppresses *BRCA2* through its 3′UTR (untranslated region) to control homologous recombination (12). But how these prostate cancer related lncRNAs are regulated or whether they contribute to prostate cancer progression is largely unknown (11–13).

In our previous work, we performed microRNA (miRNA) screening using AD and CR cells and identified a tumor suppressive miRNA, miR-99a, that is downregulated in CR cells and repressed by AR (14,15). We also showed that multiple oncogenes, *mTOR, SMARCD1, SNF2H* and *IGF1R* targeted by miR-99a contribute to prostate cancer progression (14–16). In this study, we report a novel lncRNA designated as *DRAIC* (Downregulated RNA in Androgen Independent Cells) that is similarly regulated. AR is recruited to *DRAIC* locus to repress *DRAIC*. Conversely, *DRAIC* is induced by FOXA1 and NKX3-1, which are recruited to the same region as AR at the *DRAIC* locus and FOXA1 counters the repression of *DRAIC* by AR. Interestingly, a tumor suppressive lncRNA, *PCAT29*, which was recently reported by Malik *et.al.* (13), is located 20kb downstream of *DRAIC* locus and we report that it is also regulated by AR, FOXA1 and NKX3-1 just like *DRAIC*. Functional analyses show that *DRAIC* inhibits cancer cell migration and invasion. This study indicates that progression of prostate cancer is accompanied by a decrease of FOXA1 and NKX3-1, which leads to the decrease both the novel tumor suppressive lncRNAs, *DRAIC* and *PCAT29*, thereby increasing prostate cancer migration and invasion and decreasing disease free survival. This is the first report of a novel lncRNA cluster, *DRAIC/PCAT29* regulated by the same mechanism and suppressing prostate cancer progression. Analysis of publicly available data from TCGA (The Cancer Genome Atlas) revealed that *DRAIC* is a predictor of good prognosis in at least seven other malignancies.

Materials and Methods

Cell culture

VCap cells were maintained in DMEM. PC3M-luc cells were maintained in MEM-L glutamine containing MEM Non-Essential Amino Acids, MEM Vitamin Solution, Sodium Pyruvate (All are Life technology.). Other cells were maintained in RPMI1640 medium. All medium contain 10% fetal calf serum, except when measuring the effect of androgen. For the experiments on androgen responsiveness, LNCaP cells were cultured in phenol red–free RPMI 1640 medium supplemented with charcoal:dextran-stripped FBS (Hyclone) for 48 hours before the addition of R1881 (Perkin-Elmer).

Transfection

Transfections of siRNA (50nM) and plasmid vector were performed with Lipofectamine RNAiMax and Lipofectamine 2000 (Invitrogen), respectively. siRNA sequences are shown in Supplementary Table1.

Scratch wound healing assay

Scratches were performed by pipet tip in 6 well plate. After incubation for 24h or 48h, the migration of cells into the scratch was imaged. Gap areas were calculated by Image J.

Matrigel invasion assay

Cells were seeded into 24 well Matrigel Invasion Chamber (BD Biosciences) at 1×10^5 cells in serum free medium. 10% FCS as chemoattractant was added only to the lower compartment. After incubation for 48h, the non-invaded cells were removed from the upper surface of the membrane by a cotton swab. The invaded cells were fixed using methanol, stained by Crystal Violet and counted per membrane.

RNA isolation, RT-PCR, Western Blotting and ChIP assay

Total RNA and nuclear/cytoplasmic RNAs were extracted using Trizol total RNA isolation reagent (Invitrogen), PARIS kit (Ambion), respectively. RT-PCR and Western Blotting were performed according to standard protocols. ChIP assay was performed with cells crosslinked with 1% formaldehyde and using 5 ug of antibody on Dynabeads according to published protocol (4). All details of the protocols are in Supplementary Information.

ChIP-seq analysis and RNA-seq analysis

Publicly available ChIP-seq and RNA-seq data were downloaded and analyzed by standard bioinformatics protocols. Details are described in Supplementary Information.

Kaplan-Meier plot analysis

Publicly available TCGA data at cBioPortal (17) was used to plot Kaplan-Meier plots on tumors divided into two groups based on level of *DRAIC* expressed as a Z-score (18–20) Only those plots are included that showed a statistically significant ($p<0.05$) survival difference between the two groups of patients. Similar trends were seen in other plots of these malignancies but are not included because the *p*-value did not reach significance.

Results

DRAIC is a novel lncRNA decreased in CR cells and repressed by R1881

In order to identify novel lncRNAs involved in prostate cancer progression, we compared two published RNA-sequencing (RNA-seq) datasets (21,22), [A] LNCap vs C4-2B cells and [B] vehicle vs R1881 (androgen analog)-treated LNCap cells (Fig.1A). C4-2B cells are bone metastatic CR cells derived from parental AD, LNCap cells (23). We tried to identify the lncRNAs that are (a) increased in C4-2B compared to LNCaP cells and induced by R1881 in LNCap cells or (b) decreased in C4-2B compared to LNCaP cells and repressed by R1881 in LNCap cells.

903 and 751 genes were differentially expressed ($p<0.05$) in [A] and [B] comparisons, respectively (Fig.1A). Intersection of these genes identified 72 genes that meet (a) or (b) criteria as mentioned above. Among them, there were two lncRNAs, *LOC728431* (also known as *LINC01137*) and *LOC145837*. Both were lower in C4-2B than LNCap cells and repressed by R1881 in LNCap cells (Fig.1A). *LOC728431* and *LOC145837* are composed of 3 exons at Chr.1p34.3 and 5 exons at Chr.15q23, respectively (Fig.1B).

Q-RT-PCR showed that *LOC728431* is almost at the same level in LNCap and C4-2B cells and is not drastically decreased by R1881, contrary to the RNA-seq comparisons (Fig.1C, D). Therefore we excluded *LOC728431* from further analysis.

In contrast, Q-RT-PCR confirmed that C4-2B cells express lower level of *LOC145837* (renamed by us as *DRAIC*) than LNCap cells and the expression is also decreased in other CR cells (Fig. 1E). In addition, *DRAIC* was repressed by R1881 in dose and time-dependent manners (Fig. 1F).

DRAIC is a cytoplasmic and poly-adenylated RNA

DRAIC is a spliced transcript of 1.7 kb that is expressed mainly in the cytoplasm (Supplementary Fig.1A). The coding potential (calculated by CPAT, http://rna-cpat.sourceforge.net/) of *DRAIC* is 0.342, which is comparable with those of other cytoplasmic lncRNAs: *PCAT1* (12) (0.693) (2.1 kb RNA) and *TINCR* (24) (0.204) (3.8 kb RNA). For comparison, the coding potential of protein coding genes like *GAPDH* and *Orc1* are 0.99. We confirmed the 3′end of *DRAIC* by 3′RACE using LNCap polyA+ RNA (Supplementary Fig. 1B). There are at least 3 additional transcript variants of *DRAIC* (Supplementary Fig. 2A) although RNA-seq data in LNCap cells (vehicle) (21) shows that the read counts of these 3 additional variants are much less than the ones of *DRAIC* (data not shown). Q-RT-PCR with variant-specific primers revealed that their expression patterns are similar to *DRAIC* (Supplementary Fig. 2B). There is no evidence in the 3′RACE-PCR products, the EST database or the RNAseq data of *DRAIC* being spliced to the *PCAT29* gene (13) that is located 20 kb downstream.

DRAIC is a clinically relevant lncRNA in a variety of cancers

In order to test whether Androgen Deprivation Therapy (ADT) selects for changes in expression of *DRAIC* as the cancer progresses to CR state, we analyzed published RNA-seq

of seven prostate cancer rich tumor biopsies before and after 22 weeks of ADT (25). Prostate cancer that persisted after ADT shows a 10X decrease of *DRAIC* (Fig. 2A), suggesting that androgen deprivation in patients selects for cancer cells with low expression of *DRAIC*. Note that the original publication (25) shows that only about 1600 genes are increased or decreased >2x by ADT with the vast majority of genes remaining unchanged, suggesting that the decrease of *DRAIC* was not due to a change in the lineage of cells surviving ADT.

If decreased *DRAIC* is a marker for progression of prostate cancer to CR state, one would predict that high levels of *DRAIC* may predict a good prognosis. Kaplan-Meier plot based on RNAseq and disease progression data from “Prostate Adenocarcinoma (MSKCC, 2010)” available at cBioPortal (18) revealed that lower expression of *DRAIC* predicts a lower probability of disease-free-survival of patients (Fig. 2B). Thus, *DRAIC* is a clinically relevant lncRNA that favors a good response to therapy of prostate cancer.

We wondered whether the good prognostic function of *DRAIC* could be extended to an unrelated malignancy. Kaplan-Meier plots were calculated using RNAseq and overall survival or disease-free survival data for the tumors indicated in Fig. 2C, D. Seven malignancies showed statistically significant survival benefit of *DRAIC* overeexpression in either overall survival (bladder cancer, lower grade glioma, lung adnocarcinoma) or disease free survival (renal clear cell carcinoma, hepatocellular carcinoma, skin melanoma) or both (stomach adenocarcinoma).

AR is recruited to *DRAIC* promoter and required for the repression of *DRAIC*

We next sought to identify how *DRAIC* is repressed by Androgen. The downregulation of *DRAIC* by the androgen analog, R1881, was reversed by androgen antagonist, Bicalutamide and by *AR* knockdown (Fig. 3A, B). We analyzed published AR Chromatin Immunoprecipitation-sequencing (ChIP-seq) data (26) and identified several sites upstream and within *DRAIC* that are bound by AR in the presence of R1881 (Fig. 3C). AR ChIP-PCR confirmed that AR is recruited to Regions 1, 2 and 4 by R1881 (second grey bar in each set) and that the recruitment is diminished by Bicalutamide (third grey bar in each set) (Fig. 3D). Therefore, androgen-driven AR recruitment to the *DRAIC* locus is associated with the repression.

FOXA1 and NKX3-1 occupy the same regions where AR is recruited at *DRAIC* promoter

AR often co-localizes with other transcriptional factors across the prostate genome (27). Tan PY *et.al.* showed that the binding motifs of FOXA1 and NKX3-1 are highly enriched in AR ChIP-seq samples (27). In addition, FOXA1 has been reported to act as a pioneer factor that opens local chromatin structure to allow AR to be recruited (28–31). We therefore analyzed published FOXA1 and NKX3-1 ChIP-seq datasets (26,27) to examine the binding of these transcription factors to the *DRAIC* locus (Fig. 4A, B). Interestingly, ChIP-seq peaks of these two transcriptional factors overlapped with those of AR at the *DRAIC* locus (Fig. 4A, B, Fig. 3C). We confirmed by ChIP-PCR that Regions 1, 2 and 4 bind to FOXA1 and to NKX3-1 (Fig. 4A, B). Regions 1, 2 and 4 contain several ARE (androgen-responsive element) half-

sites and several FOXA1 and NKX3-1 binding sites close to the AREs (Supplementary Fig. 3).

The expression of *DRAIC* is positively regulated by FOXA1 and NKX3-1

Contrary to our expectation that FOXA1 is a pioneer factor for AR and should repress *DRAIC*, the expression pattern of FOXA1 and NKX3-1 was similar to that of *DRAIC*: lower in most CR cells (except C4-2) compared to the AD cells (Fig. 4C and Fig. 1E). RNA-seq data from prostate adenocarcinomas from the cBioPortal (n=487) show weak but statistically significant positive correlation between the expression of *FOXA1* and *DRAIC* or *NKX3-1* and *DRAIC* (Fig. 4D, E).

In addition, knockdown of FOXA1 or NKX3-1 decreased *DRAIC* levels (Fig. 4F). The siRNA-resistant forms of *FOXA1* or *NKX3-1* partially rescued the downregulation of *DRAIC* induced by the cognate siRNAs, ruling out the possibility of off-target effects of the siRNAs (Fig. 4G). FOXA1 or NKX3-1 therefore have an opposite effect on *DRAIC* expression compared to AR, suggesting that FOXA1 is not acting as a pioneer factor for AR at the *DRAIC* promoter.

Knockdown of *FOXA1* also decreased *NKX3-1* protein and mRNA (Fig. 4F). Indeed, the *FOXA1* and *NKX3-1* mRNA levels were positively correlated in clinical samples (Fig. 4H). We did not see any significant FOXA1 ChIP-seq peaks (26) at the *NKX3-1* locus (data not shown), suggesting that FOXA1 stimulates *NKX3-1* expression by an unknown indirect mechanism.

A lncRNA, *PCAT29* is regulated by AR, FOXA1 and NKX3-1

Malik *et.al*. recently reported a tumor suppressive lncRNA, *PCAT29*, whose expression is repressed by AR (13). Interestingly, *PCAT29* gene is located 20 kb downstream of *DRAIC*. We therefore analyzed published ChIP-seq dataset for AR, FOXA1 and NKX3-1 and identified that these transcriptional factors are also recruited to *PCAT29* locus (Fig. 5A, B, C). The expression pattern of *PCAT29* in a panel of prostate cancer cells is similar to that of *DRAIC* except for C4-2B cells (Fig. 5D and Fig. 1E). Since *PCAT29* is not annotated in the level 3 data from TCGA, we used RNA from de-identified prostate cancer samples collected at UVA and used in a previous paper to analyze the correlation between *DRAIC* and *PCAT29* (14). Q-RT-PCR of these lncRNAs showed a positive correlation between the expression of the two lncRNAs (Fig. 5E). From these results, we hypothesized that *PCAT29* is regulated by FOXA1 and NKX3-1 in a manner similar to *DRAIC*. Indeed, siRNA against *FOXA1* or *NKX3-1* decreased *PCAT29* expression (Fig. 5F, Fig. 4F).

Jin *et.al*. recently reported that FOXA1 knockdown can shift or increase AR binding to selected sites (30). We analyzed their AR ChIP-seq data and found that sh*FOXA1* increases AR recruitment at *DRAIC/PCAT29* cluster (Fig. 5G). Thus, FOXA1 actually decreases the recruitment of AR to the *DRAIC/PCAT29* locus. Consistent with this, R1881 treatment or FOXA1 knockdown independently repress *DRAIC* and *PCAT29*, but together they repress both genes even further (Fig. 5H). This result suggests that instead of being a pioneer factor of AR, *FOXA1* counters the action of AR at the *DRAIC/PCAT29* cluster.

DRAIC represses cellular migration and invasion

Like *PCAT29* (13), *DRAIC* is a marker for good prognosis in prostate cancer (Fig. 2B), and so is expected to repress oncogenic phenotypes. *PCAT29* has been reported to repress invasion and metastasis (13). The ability of a panel of prostate cancer cells to invade through Matrigel in a Boyden Chamber assay was anti-correlated with the level of expression of *DRAIC* in the same cells (Fig. 6A; Fig. 1E), suggesting that *DRAIC*, like *PCAT29*, represses invasion. Transient knockdown of *DRAIC* by siRNA in LNCap cells unexpectedly decreased cell numbers by about 30-50% (Fig. 6B), suggesting that *DRAIC* has a pro-proliferative function. When *DRAIC* was stably knocked down by shRNA in LNCap cells, the cell proliferation was similarly decreased (data not shown) but interestingly, the cell morphology was changed from cuboidal to fibroblast-like shape (Fig. 6C). Stable *DRAIC* overexpression in PC3M-luc cells, in contrast, showed the opposite phenotype, with a change in morphology from fibroblast shape to cuboidal shape (Fig. 6D). In a scratch assay to measure cell migration and in a Matrigel invasion assay, the migration and invasion of LNCaP cells is increased by *DRAIC* knockdown (Fig. 6E, F). In similar assays, the migration and invasion of PC3M-luc cells is decreased by *DRAIC* overexpression (Fig. 6G, H). Taken together, these results suggest that *DRAIC* promotes cell proliferation but inhibits cell migration and invasion. We summarized the similarities and differences between *DRAIC* and *PCAT29* in Figure 7A.

Discussion

The regulation of *DRAIC* and *PCAT29* genes is remarkably similar to that we reported for the miR-99 family (14,15). AR is recruited to the pri-*miR-99a* promoter and represses transcription in concert with EZH2 (14,15). Considering that AR is recruited to broad regions around *DRAIC* (and the transcript variants) and *PCAT29* gene, it is conceivable that a chromatin looping mechanism following AR recruitment is involved to produce a large domain with gene suppression.

FOXA1 and NKX3-1 have been variably thought to be tumor suppressive (32,33) and oncogenic (34,35). In the regulation described here, the two factors appear to be tumor suppressive in that their levels are decreased in CR cells and they are positive transcription factors for *DRAIC* and *PCAT29*, both of which decrease migration and invasion and predict good prognosis. We propose a model that FOXA1 and NKX3-1 induce the expression of *DRAIC/PCAT29* in AD prostate epithelial cells but are downregulated in CR cells, leading to the decrease of *DRAIC* (Fig. 7B). Moreover, *DRAIC* is further repressed in the CR cells by differently activated androgen-responsive pathways (Fig. 7B).

FOXA1 is well known to be a pioneer factor and stimulates AR-mediated gene regulation (28–31). But our study clearly shows that FOXA1 counters the repression of *DRAIC/PCAT29* by AR (Fig. 5H). Jin *et. al.* showed that excess of FOXA1 opens up an excess of chromatin regions and ends up diluting AR across the genome thereby indirectly inhibiting specific AR binding events (30). Therefore we need to study whether FOXA1 directly or indirectly represses AR recruitment to *DRAIC/PCAT29* cluster. Similarly, NKX3-1 is known to be positively regulated by AR and facilitates regulation of the AR downstream

genes by associating with AR (27). However, at the *DRAIC/PCAT29* locus NKX3-1 has the opposite effect of AR on gene expression, suggesting a different mode of action.

Our functional analysis showed that *DRAIC* represses migration and invasion (Fig. 6) just like *PCAT29* (13). However, knockdown of *DRAIC* represses cell proliferation (Fig. 6B) while knockdown of *PCAT29* induces proliferation (13), suggesting that all functions of these lncRNA are not identical. This is borne out by the different cellular localization of *DRAIC* (cytoplasmic) and *PCAT29* (nuclear) (13). Future studies will analyze whether *DRAIC* and *PCAT29* synergize with each other in repressing cell migration and invasion *in vitro* and *in vivo*.

Although it is tempting to propose that *DRAIC* represses epithelial-mesenchymal transition (EMT), preliminary results suggest that levels of mRNA involved in EMT are unchanged by *DRAIC* knockdown or overexpression (data not shown). Diverse mechanisms have been proposed by which lncRNAs could regulate many phenotypes at transcriptional and post-transcriptional levels (36). Thus a detailed analysis is needed to determine the downstream targets of this cytoplasmic lncRNA and the molecular mechanism by which *DRAIC* regulates cellular migration and invasion.

It will be interesting to investigate in the future whether *DRAIC/PCAT29* expression levels are related to the Gleason grade and whether they are useful as an independent prognostic biomarkers of prostate cancer. The results reported here highlight that a thorough study of lncRNAs altered during prostate cancer genesis and progression will be very important for improving our understanding and the therapy of this cancer.

Finally, *DRAIC* expression predicts good prognosis in a wide range of malignancies from many other tissues, suggesting that it is an important and ubiquitous tumor suppressor. Whether the mechanism by which clinical progression is suppressed is the same in all these tumors, and whether *PCAT29* has a similar anti-progression effect in these tumors as in prostate cancer, will be important questions for the future.

Supplementary Material

Refer to Web version on PubMed Central for supplementary material.

Acknowledgments

We thank members of the Prostate Cancer Research Working group at UVA and the Dutta laboratory for advice and helpful discussions.

Financial support: This work was supported by P01CA104106 from NIH to AD

References

1. Karantanos T, Corn PG, Thompson TC. Prostate cancer progression after androgen deprivation therapy: mechanisms of castrate resistance and novel therapeutic approaches. Oncogene. 2013; 32:5501–11. [PubMed: 23752182]
2. Chen CD, Welsbie DS, Tran C, Baek SH, Chen R, Vessella R, et al. Molecular determinants of resistance to antiandrogen therapy. Nat Med. 2004; 10:33–9. [PubMed: 14702632]

3. Majumder PK, Sellers WR. Akt-regulated pathways in prostate cancer. Oncogene. 2005; 24:7465–74. [PubMed: 16288293]
4. Negishi M, Wongpalee SP, Sarkar S, Park J, Lee KY, Shibata Y, et al. A new lncRNA, APTR, associates with and represses the CDKN1A/p21 promoter by recruiting polycomb proteins. PLoS One. 2014; 9:e95216. [PubMed: 24748121]
5. Dey BK, Pfeifer K, Dutta A. The H19 long noncoding RNA gives rise to microRNAs miR-675-3p and miR-675-5p to promote skeletal muscle differentiation and regeneration. Genes Dev. 2014; 28:491–501. [PubMed: 24532688]
6. Mueller AC, Cichewicz Ma, Dey BK, Layer R, Reon BJ, Gagan JR, et al. MUNC: A lncRNA that induces the expression of pro-myogenic genes in skeletal myogenesis. Mol Cell Biol. 2014 in press.
7. Kumar P, Anaya J, Mudunuri SB, Dutta A. Meta-analysis of tRNA derived RNA fragments reveals that they are evolutionarily conserved and associate with AGO proteins to recognize specific RNA targets. BMC Biol. 2014; 12:78. [PubMed: 25270025]
8. Cesana M, Cacchiarelli D, Legnini I, Santini T, Sthandier O, Chinappi M, et al. A long noncoding RNA controls muscle differentiation by functioning as a competing endogenous RNA. Cell. 2011; 147:358–69. [PubMed: 22000014]
9. Yuan J, Yang F, Wang F, Ma J, Guo Y, Tao Q, et al. A long noncoding RNA activated by TGF-β promotes the invasion-metastasis cascade in hepatocellular carcinoma. Cancer Cell. 2014; 25:666–81. [PubMed: 24768205]
10. Wahlestedt C. Targeting long non-coding RNA to therapeutically upregulate gene expression. Nat Rev Drug Discov. 2013; 12:433–46. [PubMed: 23722346]
11. Yang L, Lin C, Jin C, Yang JC, Tanasa B, Li W, et al. lncRNA-dependent mechanisms of androgen-receptor-regulated gene activation programs. Nature. 2013; 500:598–602. [PubMed: 23945587]
12. Prensner JR, Chen W, Iyer MK, Cao Q, Ma T, Han S, et al. PCAT-1, a long noncoding RNA, regulates BRCA2 and controls homologous recombination in cancer. Cancer Res. 2014; 74:1651–60. [PubMed: 24473064]
13. Malik R, Patel L, Prensner JR, Shi Y, Iyer MK, Subramaniyan S, et al. The lncRNA PCAT29 Inhibits Oncogenic Phenotypes in Prostate Cancer. Mol Cancer Res. 2014; 12:1081–7. [PubMed: 25030374]
14. Sun D, Lee YS, Malhotra A, Kim HK, Matecic M, Evans C, et al. miR-99 family of MicroRNAs suppresses the expression of prostate-specific antigen and prostate cancer cell proliferation. Cancer Res. 2011; 71:1313–24. [PubMed: 21212412]
15. Sun D, Layer R, Mueller aC, Cichewicz Ma, Negishi M, Paschal BM, et al. Regulation of several androgen-induced genes through the repression of the miR-99a/let-7c/miR-125b-2 miRNA cluster in prostate cancer cells. Oncogene. 2014; 33:1448–57. [PubMed: 23503464]
16. Mueller, aC; Sun, D.; Dutta, a. The miR-99 family regulates the DNA damage response through its target SNF2H. Oncogene. 2013; 32:1164–72. [PubMed: 22525276]
17. Cerami E, Gao J, Dogrusoz U, Gross BE, Sumer SO, Aksoy BA, et al. The cBio cancer genomics portal: an open platform for exploring multidimensional cancer genomics data. Cancer Discov. 2012; 2:401–4. [PubMed: 22588877]
18. Taylor BS, Schultz N, Hieronymus H, Gopalan A, Xiao Y, Carver BS, et al. Integrative genomic profiling of human prostate cancer. Cancer Cell. 2011; 18:11–22. [PubMed: 20579941]
19. Weinstein JN, Akbani R, Broom BM, Wang W, Verhaak RG, McConkey D, et al. Comprehensive molecular characterization of urothelial bladder carcinoma. Nature. 2014; 507:315–22. [PubMed: 24476821]
20. Collisson, Ea; Campbell, JD.; Brooks, AN.; Berger, AH.; Lee, W.; Chmielecki, J., et al. Comprehensive molecular profiling of lung adenocarcinoma. Nature. 2014; 511:543–50. [PubMed: 25079552]
21. Decker KF, Zheng D, He Y, Bowman T, Edwards JR, Jia L. Persistent androgen receptor-mediated transcription in castration-resistant prostate cancer under androgen-deprived conditions. Nucleic Acids Res. 2012; 40:10765–79. [PubMed: 23019221]

22. Tewari AK, Yardimci GG, Shibata Y, Sheffield NC, Song L, Taylor BS, et al. Chromatin accessibility reveals insights into androgen receptor activation and transcriptional specificity. Genome Biol. 2012; 13:R88. [PubMed: 23034120]
23. Thalmann GN, Anezinis PE, Chang S, Thaimann N, Hopwood VL, Pathak S, et al. Androgen-independent Cancer Progression and Bone Metastasis in the LNCaP Model of Human Prostate Cancer Model of Human Prostate Cancer. Cancer Res. 1994; 54:2577–81. [PubMed: 8168083]
24. Kretz M, Siprashvili Z, Chu C, Webster DE, Zehnder A, Qu K, et al. Control of somatic tissue differentiation by the long non-coding RNA TINCR. Nature. 2013; 493:231–5. [PubMed: 23201690]
25. Rajan P, Sudbery IM, Villasevil MEM, Mui E, Fleming J, Davis M, et al. Next-generation sequencing of advanced prostate cancer treated with androgen-deprivation therapy. Eur Urol. 2014; 66:32–9. [PubMed: 24054872]
26. Yu J, Yu J, Mani RS, Cao Q, Brenner CJ, Cao X, et al. An integrated network of androgen receptor, polycomb, and TMPRSS2-ERG gene fusions in prostate cancer progression. Cancer Cell. 2010; 17:443–54. [PubMed: 20478527]
27. Tan PY, Chang CW, Chng KR, Wansa KDSA, Sung WK, Cheung E. Integration of regulatory networks by NKX3-1 promotes androgen-dependent prostate cancer survival. Mol Cell Biol. 2012; 32:399–414. [PubMed: 22083957]
28. Cai C, He HH, Gao S, Chen S, Yu Z, Gao Y, et al. Lysine-Specific Demethylase 1 Has Dual Functions as a Major Regulator of Androgen Receptor Transcriptional Activity. Cell Rep. 2014; 9:1618–27. [PubMed: 25482560]
29. Robinson JLL, Hickey TE, Warren aY, Vowler SL, Carroll T, Lamb aD, et al. Elevated levels of FOXA1 facilitate androgen receptor chromatin binding resulting in a CRPC-like phenotype. Oncogene. 2014; 33:5666–74. [PubMed: 24292680]
30. Jin HJ, Zhao JC, Wu L, Kim J, Yu J. Cooperativity and equilibrium with FOXA1 define the androgen receptor transcriptional program. Nat Commun. 2014; 5:3972. [PubMed: 24875621]
31. Mills IG. Maintaining and reprogramming genomic androgen receptor activity in prostate cancer. Nat Rev Cancer. 2014; 14:187–98. [PubMed: 24561445]
32. Jin HJ, Zhao JC, Ogden I, Bergan RC, Yu J. Androgen receptor-independent function of FoxA1 in prostate cancer metastasis. Cancer Res. 2013; 73:3725–36. [PubMed: 23539448]
33. Bowen C, Bubendorf L, Voeller HJ, Progression T, Slack R, Willi N, et al. Loss of NKX3.1 Expression in Human Prostate Cancers Correlates with Tumor Progression. Cancer Res. 2000; 60:6111–5. [PubMed: 11085535]
34. Gerhardt J, Montani M, Wild P, Beer M, Huber F, Hermanns T, et al. FOXA1 promotes tumor progression in prostate cancer and represents a novel hallmark of castration-resistant prostate cancer. Am J Pathol. 2012; 180:848–61. [PubMed: 22138582]
35. Xu LL, Srikantan V, Sesterhenn IA, Augustus M, Dean R, Moul JW, et al. Expression profile of an androgen regulated prostate specific homeobox gene NKX3.1 in primary prostate cancer. J Urol. 2000; 163:972–9. [PubMed: 10688034]
36. Dey BK, Mueller AC, Dutta A. Long non-coding RNA as emerging regulators of differentiation, development, and disease. Transcription. 2014 in press.

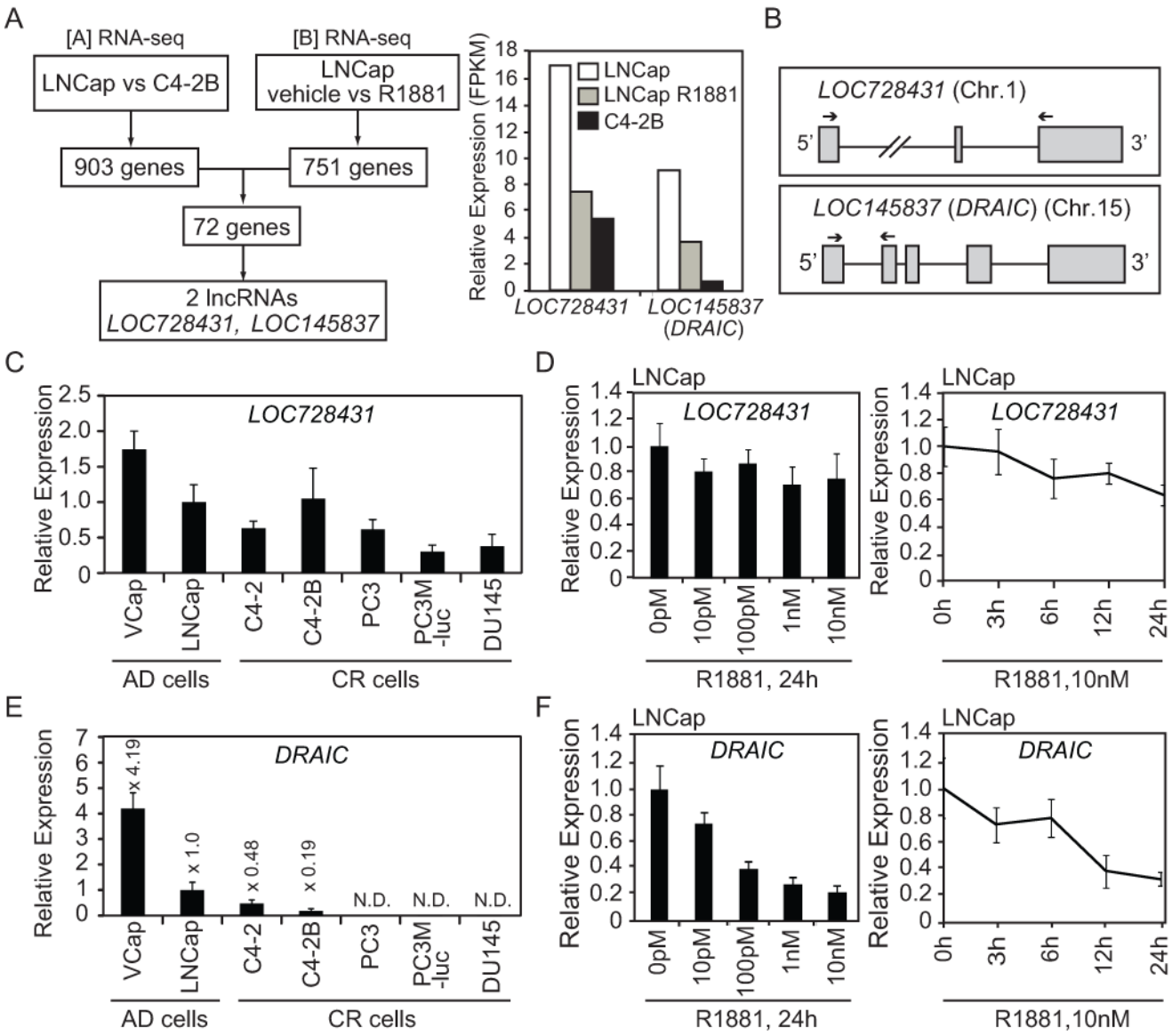

Figure 1. LncRNA, *DRAIC* is downregulated in CR cells and decreased by R188

(A) Left: analysis of published RNA-seq datasets. Right: Relative expression (FPKM: Fragments Per Kilobase of exon per Million fragments mapped) of *LOC728431* and *LOC145837* (*DRAIC*) in LNCap cells treated with vehicle or R1881 and C4-2B cells treated with vehicle (B) Top and bottom show *LOC728431* and *LOC145837* (*DRAIC*) gene structures and qPCR primer locations, respectively. (C) The expression of *LOC728431* in a panel of prostate cancer cells cultured in the growth medium was measured by RT-qPCR and normalized to *GAPDH*. Mean±S.D. n=3. The expression in LNCap is set as 1. (D) LNCap cells were treated with R1881 at different doses (left) and times (right) and the expression of *LOC728431* was measured by RT-qPCR. The expression in 0 pM or 0 h is set as 1. Rest as in Fig. 1C. (E) The expression of *DRAIC* in a panel of prostate cancer cells cultured in growth medium was measured by RT-qPCR. Rest as in Fig. 1C. (F) LNCap cells

were treated with R1881 at different doses (left) and times (right) and the expression of *DRAIC* was measured by RT-qPCR. Rest as in Fig. 1C, D.

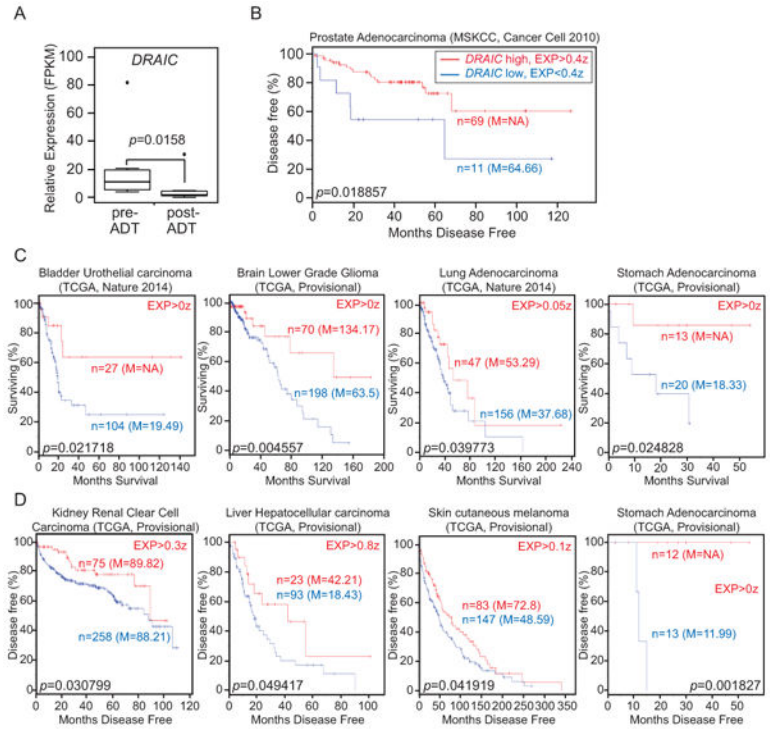

Figure 2. *DRAIC* is a clinically relevant lncRNA

(A) Relative expression (FPKM) of *DRAIC* in prostate cancer pre- and post-ADT (Androgen Deprivation Therapy) (post-ADT: prostate cancer harvested approximately 22 weeks after ADT initiation) using published RNA-seq dataset from 7 patients (25). The expression of *DRAIC* was determined using the Tuxedo suite and plotted using R. The statistical significance of the changes in *DRAIC* expression was evaluated using a paired t-test. p=0.0158. (B). Kaplan–Meier plot of disease-free survival (DFS) of patient with prostate adenocarcinoma from the MSKCC dataset (18) stratified by level of *DRAIC* expression. In Log rank test p=0.018857. High: *DRAIC* level > +0.4z and Low: *DRAIC* level < +0.4z. (C and D) Kaplan–Meier plot of Overall survival (OS) (C) or Disease Free Survival (D) for indicated malignancies from TCGA (19,20) stratified by level of *DRAIC* expression. EXP: the *DRAIC* expression level z-score cut-off used for dividing high expressers from low expressers. n = number of patients in that group, M = median survival in months of that group. NA: not available.

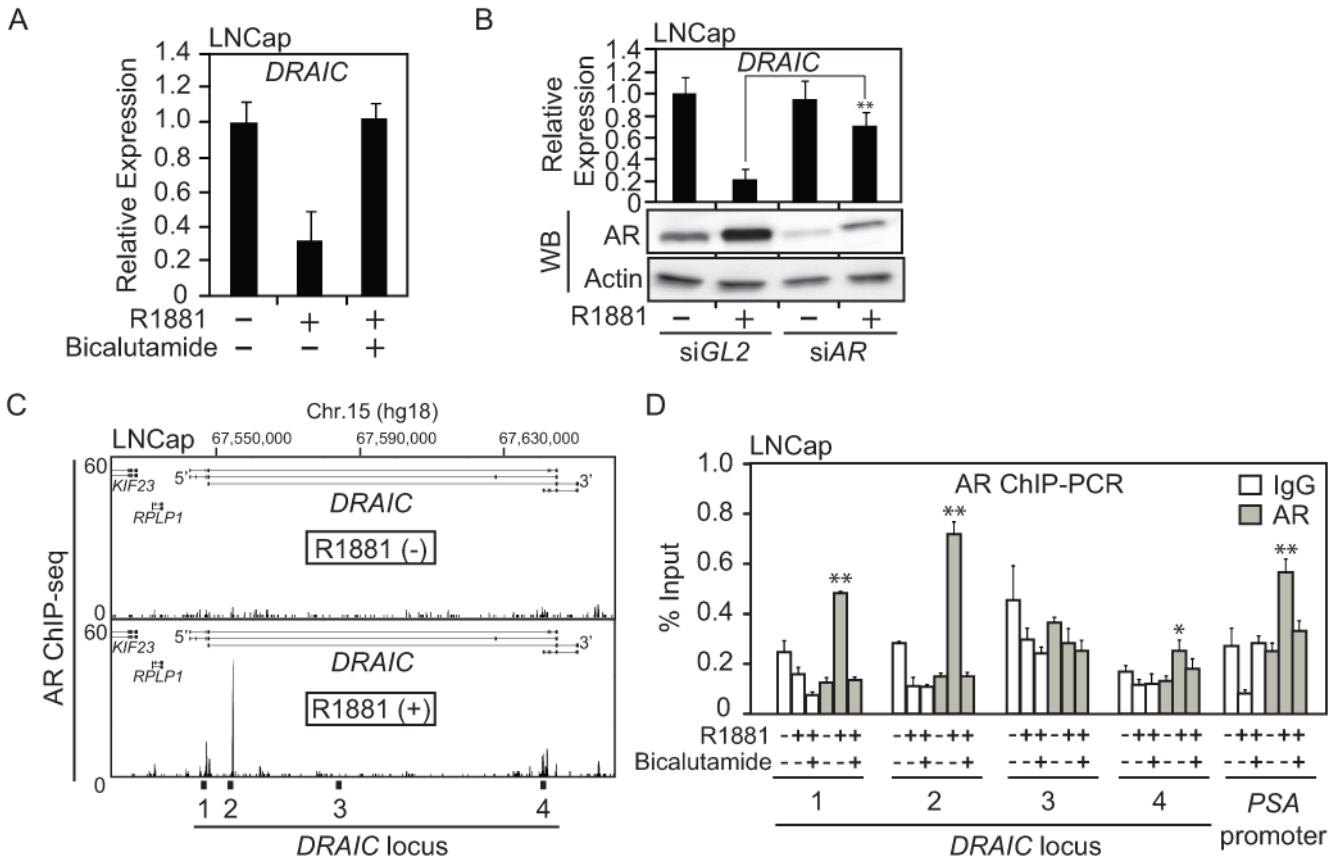

Figure 3. AR is recruited to *DRAIC* locus and required for *DRAIC* downregulation

(A) LNCaP cells were treated with no androgen, 10 nM R1881, 10 nM R1881 plus 10 uM Bicalutamide for 24h. The expression of *DRAIC* in LNCaP cells was measured by RT-qPCR and normalized to *GAPDH*. Rest as in Fig. 1C. (B) The expression of *DRAIC* in LNCaP cells after knocking down AR by siRNA for 72 h in the absence or presence of 10 nM R1881 for 24h. ** indicates *p*-value of difference from si*GL2* < 0.01. Rest as in Figure 1C. The expression of AR and Actin (loading control) were detected by western blotting. (C) Published AR ChIP-seq (26) peaks in LNCap cells at *DRAIC* locus in the absence (upper) or presence (lower) of R1881. Regions 1-4 in the *DRAIC* locus are marked. (D) LNCap cells were treated with or without 10 nM R1881 and 10uM Bicalutamide for 24h and AR ChIP-PCR performed. *PSA* promoter was used as a positive control (15) and region 3 was used as a negative control. The value was expressed as percentage of input DNA. ** and * indicate *p*-value <0.01, 0.05, respectively.

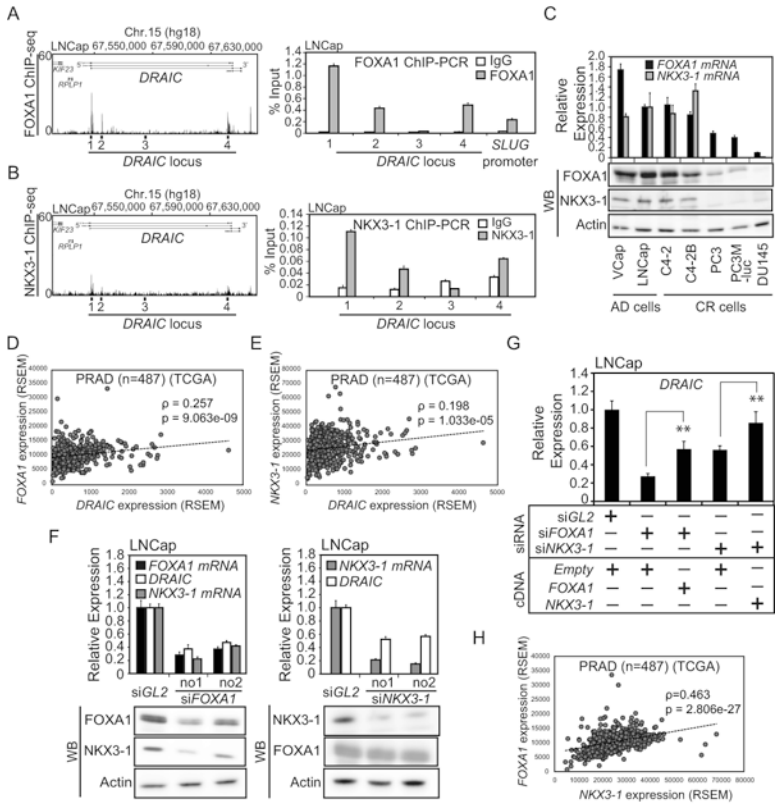

Figure 4. FOXA1 and NKX3-1 positively regulate *DRAIC*

(A) Left: Published FOXA1 ChIP-seq (26) peaks in LNCap cells cultured in the growth medium. Right: FOXA1 ChIP-PCR was performed with cells in 10% FCS. *SLUG* promoter was used as a positive control (32). Rest as in Fig. 3D. (B) Left: Published NKX3-1 ChIP-seq (27) peaks in LNCap cells treated with Dihydrotestosterone (DHT). Rgith: NKX3-1 ChIP-PCR was performed with cells in 10% FCS. Rest as in Fig. 3D. (C) The mRNA and protein levels of *FOXA1* and *NKX3-1* were measured by RT-qPCR and western blotting, respectively. Rest as in Fig. 1C. (D and E) The correlation of levels of *DRAIC* and *FOXA1* or *DRAIC* and *NKX3-1* RNAs in prostate adenocarcinoma (PRAD) samples (n=487) from tier-3 RNA-seq data of TCGA. Spearman correlation coefficients and *p*-values are shown. (F) LNCap cells cultured in growth medium were transfected with siRNA against *FOXA1*, *NKX3-1* or si*GL2* for 72h. The RNA levels of *DRAIC*, *FOXA1* and *NKX3-1* and the protein levels of FOXA1, NKX3-1 and Actin were measured by RT-qPCR and western blotting, respectively. In RT-qPCR, the expression in si*GL2* is set as 1. Rest as in Fig. 1C. (G) LNCap cells cultured in the growth medium were transfected with siRNA against *FOXA1* no.1, *NKX3-1* no.1 or si*GL2* and 3μg expression vector of pcDNA3-*FOXA1*, -*NKX3-1* or -*Empty* for 72 h. The expression of *DRAIC* was measured by RT-qPCR. The expression of *DRAIC* in si*GL2* plus *Empty* vector cells is set as 1. ** indicates *p*-value<0.01. Rest as in Fig. 1C. (H) The correlation curve between *FOXA1* and *NKX3-1* RNAs in prostate adenocarcinoma (PRAD) samples (n=487). Rest as in Fig.4D, E.

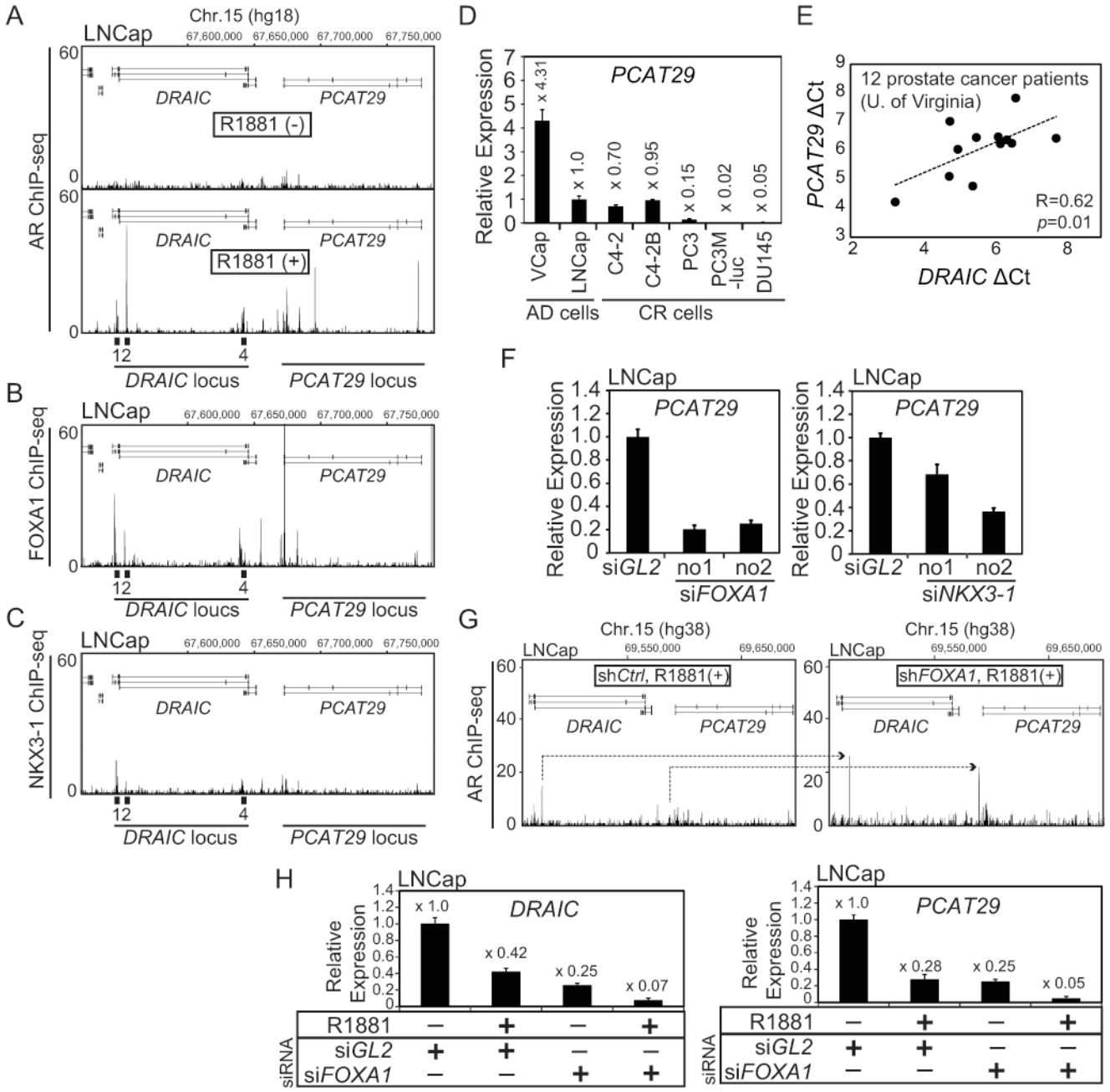

Figure 5. A neighboring lncRNA, *PCAT29* is also repressed by AR and activated by FOXA1 and NKX3-1

(A) Published AR ChIP-seq (26) peaks in LNCap cells at *DRAIC* and *PCAT29* loci in the absence (upper) or presence (lower) of R1881. (B) Published FOXA1 ChIP-seq (26) peaks in LNCap cells cultured in the growth medium at *DRAIC* and *PCAT29* loci. (C) Published NKX3-1 ChIP-seq (27) peaks in LNCap cells treated with Dihydrotestosterone (DHT) at *DRAIC* and *PCAT29* loci. (D) The expression of *PCAT29* in a panel of prostate cancer cells was measured by RT-qPCR. Rest as in Fig. 1C. (E) The delta Ct values of *DRAIC* and *PCAT29* (normalized to *GAPDH*) in 12 prostate cancer patients (University of Virginia)

were subjected to Pearson correlation analysis. (F) The expression of *PCAT29* after transfection of siRNA against *FOXA1*, *NKX3-1* or si*GL2* was measured by RT-qPCR. Rest as in Fig. 4F. (G) Published AR ChIP-seq results (30) show induction of AR binding (arrows) at *DRAIC* and *PCAT29* loci in LNCap cells treated with sh*FOXA1* or sh*Ctrl* (negative control). R1881 is present in both cultures. (H) LNCap cells were treated with si*GL2* or si*FOXA1* for 72h in the absence or presence of R1881 (10 nM) for 24h. The expression of *DRAIC* (Left) and *PCAT29* (Right) are measured by RT-qPCR. The expression in si*GL2*/R1881 (-) is set as 1. Rest as in Fig. 1C.

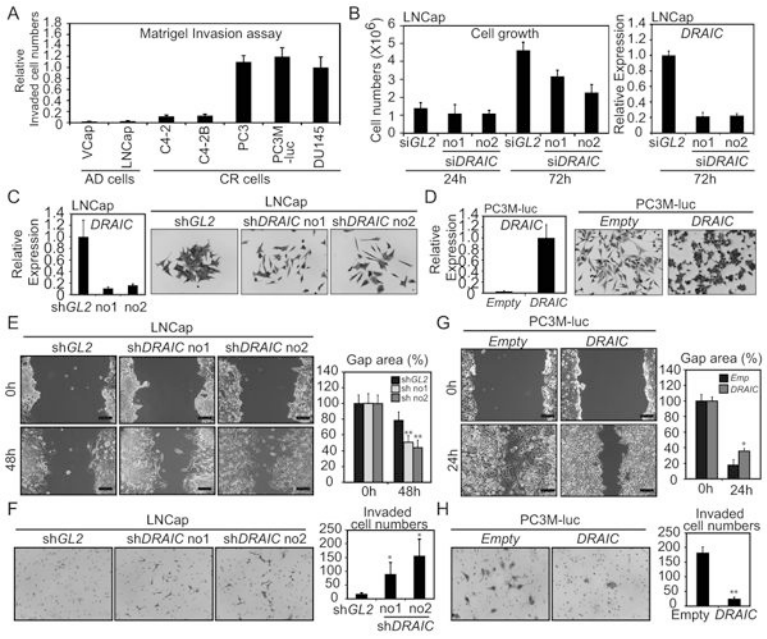

Figure 6. *DRAIC*represses cancer cell migration and invasion

(A) The relative number of cells invaded through matrigel is normalized to number in DU145 cells. (B) Left; Proliferation of LNCap cells after transfection of siRNAs. Right; *DRAIC* RNA measured by RT-qPCR and normalized to *GAPDH*. Rest as in Fig. 1C. (C) LNCap transduced with lentivirus expressing sh*GL2*, -sh*DRAIC* no1 or no2. Left: *DRAIC* mRNA normalized to *GAPDH*. Rest as in Fig. 1C. Right: Cells stained by Crystal Violet. (D) PC3M-luc cells stably transfected with pcDNA3-*DRAIC* or pcDNA3-*Empty*. Left: *DRAIC* RNA normalized to *GAPDH*. The level in *DRAIC* overexpressing cells is set as 1. Rest as in Fig. 1C. (E) Scratch wound healing assay with LNCap cells stably expressing sh*GL2* or sh*DRAIC*. Left: Representative images of scratch shown. Scale bar: 20μm. Right: gap area quantitated by Image J. Mean±S.D. n=5. ** : difference from sh*GL2* $p<0.01$. (F) Matrigel Invasion assay with LNCap expressing sh*GL2* or sh*DRAIC*. Left: Invaded cells fixed in methanol, stained by Crystal Violet. Right: Number of invaded cells. Rest as in (E). (G) Scratch wound healing assay with *Empty* or *DRAIC* overexpressing PC3M-luc cells. Image and bar graph as in (E) *: difference from *Empty* $p<0.05$. (H) Matrigel invasion assay was performed using *Empty* or *DRAIC* overexpressing PC3M-luc cells. Rest as in (F).

A

	DRAIC	*PCAT29*
transcript size	1702bp	694bp
poly adenylation	Yes	Yes
cellular localization	cytoplasm	nuclear
Kaplan Meier plot	MSKCC, Cancer Cell, 2010 good prognostic marker	University of Michigan good prognostic marker
negative regulator	AR	AR
positive regulator	FOXA1, NKX3-1	FOXA1, NKX3-1
cell growth	induce	repress
migration, invasion	repress	repress

B

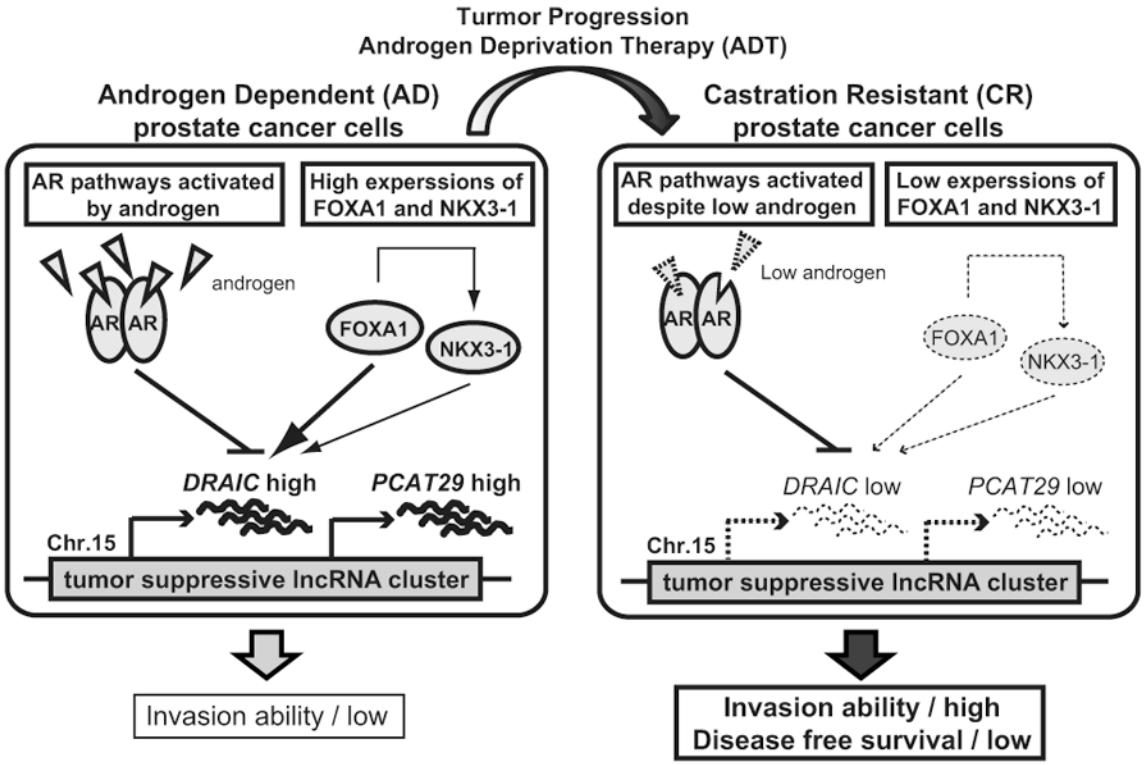

Figure 7. Schematic representation of the proposed regulation of lncRNA cluster, *DRAIC/PCAT29*

(A) Comparison of *DRAIC* and *PCAT29*. (B) In AD cells, even though AR activated by androgen is recruited to *DRAIC/PCAT29* cluster to repress these two lncRNA, the high level of FOXA1 counters the repression of *DRAIC/PCAT29* by AR and induces the transcription of these lncRNAs. NKX3-1, which is indirectly up-regulated by FOXA1, contributes to the induction of *DRAIC/PCAT29*. During tumor progression, the expression of FOXA1 and NKX3-1 is downregulated and AR pathways are differentially activated despite low

androgen in CR cells. The decrease of FOXA1 enhances AR recruitment to the cluster and represses *DRAIC/PCAT29*. ADT selects for cells with decreased *DRAIC* expression. The decrease of tumor suppressive lncRNAs, *DRAIC* and *PCAT29*, leads to higher invasion ability and lower disease free survival in prostate cancer patients.